SUPPORTING INFORMATION

Structural and magnetic variations in tetranuclear Ni^{II} clusters: the effect of the reaction solvent and ligand substitution on the product identity

Panagiota S. Perlepe,[a,b] Angeliki A. Athanasopoulou,[a] Konstantina I. Alexopoulou,[b] Catherine P. Raptopoulou,[c] Vassilis Psycharis,[c] Albert Escuer,[d] Spyros P. Perlepes*[b] and Theocharis C. Stamatatos*[a]

[a] *Department of Chemistry, 500 Glenridge Ave, Brock University, L2S 3A1 St. Catharines, Ontario, Canada.*

[b] *Department of Chemistry, University of Patras, 265 04 Patras, Greece.*

[c] *Institute of Advanced Materials, Physicochemical Processes, Nanotechnology and Microsystems, NCSR "Demokritos", 153 10 Agia Paraskevi Attikis, Greece.*

[d] *Departament de Quimica Inorganica, Universitat de Barcelona, Diagonal 645, 08028 Barcelona, Spain.*

---

* To whom correspondence should be addressed: E-mail: tstamatatos@brocku.ca (Th.C.S.)

Experimental Section

Syntheses. All manipulations were performed under aerobic conditions using materials as received. The organic ligands samphH_2 (orange crystalline solid) and sacbH_2 (yellow crystalline solid) were synthesized by following a well-known synthetic protocol for the synthesis of similar Schiff base ligands. This includes the condensation in refluxing absolute methanol of 2-amino-4-methylphenol or 2-amino-5-chlorobenzoic acid[1] with salicylaldehyde, in accordance with literature methods for the similar ligand saphH_2.[2] Large green crystals of the $[Ni_2(H_2O)(O_2CBu^t)_4(HO_2CBu^t)_4]$ precursor were obtained in 70% yield by following a previously described synthetic route.[3]

$[Ni_4(samph)_4(EtOH)_4]$ (1): To a stirred, yellow solution of samphH_2 (0.02 g, 0.10 mmol) in EtOH (10 mL) was added a green solution of $[Ni_2(H_2O)(O_2CBu^t)_4(HO_2CBu^t)_4]$ (0.05 g, 0.05 mmol) in the same solvent (10 mL). The resulting brown solution was stirred for 15 min, filtered, and left undisturbed to slowly evaporate at room temperature. After three days, X-ray quality olive-green plate-like crystals of **1**·0.7EtOH had appeared and were collected by filtration, washed with cold EtOH (2 x 2 mL) and Et_2O (2 x 3 mL), and dried in air. The yield was 35%. Anal. Calcd (Found) for **1** (lattice solvent-free): C 58.23 (58.17), H 5.19 (5.02), N 4.24 (4.36). CCDC deposition number: 1018616. Selected IR data (KBr): ν= 2920 (mb), 1602 (vs), 1532 (m), 1490 (vs), 1464 (s), 1440 (s), 1380 (m), 1340 (w), 1308 (m), 1244 (m), 1224 (m), 1186 (m), 1148 (m), 1126 (m), 1038 (m), 912 (w), 826 (m), 754 (m), 556 (m), 528 (m), 454 (w).

$[Ni_4(samph)_4(DMF)_2]$ (2): To a stirred, green suspension of $[Ni_2(H_2O)(O_2CBu^t)_4(HO_2CBu^t)_4]$ (0.05 g, 0.05 mmol) in DMF (5 mL) was added a yellow solution of samphH_2 (0.02 g, 0.10 mmol) in the same solvent (5 mL). The resulting dark orange solution was stirred for 15 min, filtered, and left undisturbed to slowly evaporate at room temperature. After three days, X-ray quality orange plate-like crystals of **2**·2DMF had appeared and were collected by filtration, washed with cold DMF (1 x 2 mL) and Et_2O (2 x 3 mL), and dried under vacuum. The yield was

---

[1] A. A. Athanasopoulou, C. P. Raptopoulou, A. Escuer and Th. C. Stamatatos, *RSC Adv.*, 2014, **4**, 12680.

[2] A. Kagkelari, G. S. Papaefstathiou, C. P. Raptopoulou and T. F. Zafiropoulos, *Polyhedron*, 2009, **28**, 3279.

[3] G. Chaboussant, R. Basler, H.- U. Güdel, S. Ochsenbein, A. Parkin, S. Parsons, G. Rajaraman, A. Sieber, A. A. Smith, G. A. Timco and R. E. P. Winpenny, *Dalton Trans.*, 2004, 2758.

40%. Anal. Calcd (Found) for **2**·DMF: C 57.62 (57.87), H 4.84 (4.98), N 7.24 (7.05). CCDC deposition number: 1018617. IR data (KBr): *ν*= 3444 (mb), 2922 (m), 1666 (vs), 1650 (vs), 1600 (vs), 1540 (w), 1528 (m), 1492 (s), 1472 (m), 1438 (s), 1376 (m), 1350 (w), 1326 (w), 1298 (m), 1280 (m), 1256 (m), 1226 (m), 1190 (m), 1160 (w), 1142 (m), 1124 (m), 1104 (w), 1090 (m), 1044 (w), 912 (w), 862 (w), 828 (s), 758 (m), 680 (m), 656 (w), 618 (w), 584 (w), 522 (m), 486 (m), 456 (w).

[Ni_4(sacb)$_4$(EtOH)$_4$] (3): To a stirred, yellow solution of sacbH_2 (0.06 g, 0.20 mmol) in EtOH (20 mL) was added solid [$Ni_2(H_2O)(O_2CBu^t)_4(HO_2CBu^t)_4$] (0.10 g, 0.10 mmol). The resulting green-yellow mixture was stirred for 20 min, during which time all the solids dissolved and the color of the solution changed to dark green. The solution was filtered and the filtrate was left to evaporate slowly at room temperature. After four days, X-ray quality green plate-like crystals of **3**·6EtOH had appeared and were collected by filtration, washed with cold EtOH (2 x 2 mL) and Et_2O (2 x 3 mL), and dried in air. The yield was 60%. Anal. Calcd (Found) for **3**·2EtOH: C 50.86 (50.97), H 4.27 (4.41), N 3.49 (3.24). CCDC deposition number: 1018618. Selected IR data (KBr): *ν*= 3299 (mb), 1579 (vs), 1550 (s), 1462 (s), 1439 (s), 1409 (s), 1358 (s), 1287 (m), 1177 (m), 1151 (m), 1117 (m), 1042 (m), 984 (w), 925 (m), 895 (m), 846 (m), 742 (m), 592 (w), 460 (w).

Synthetic hint! The reaction that led to complex **3** has been repeated in DMF (instead of EtOH) under exactly the same conditions. The resulting orange solution afforded a yellow oily product which was recrystallized from various organic solvents (polar and apolar, protic and aprotic). Only when EtOH was employed as the recrystallization solvent we have been able to isolate a microcrystalline material, and that was identified as complex **3**.

SINGLE-CRYSTAL X-RAY CRYSTALLOGRAPHY

X-ray Crystal Structure Determinations

Crystals of complexes **1**·0.7EtOH (0.13 x 0.19 x 0.38 mm) and **2**·2DMF (0.05 x 0.11 x 0.22 mm) were taken from the mother liquor and immediately cooled at -113 ^{o}C. Diffraction measurements were made on a Rigaku R-AXIS SPIDER Image Plate diffractometer using graphite-monochromated Cu Kα radiation. Data collection (ω-scans) and processing (cell refinement, data reduction and empirical absorption correction) were performed using the CrystalClear program package.[4] A crystal of **3**·6EtOH (0.03 x 0.12 x 0.13 mm) was taken from the mother liquor and immediately cooled at -123 ^{o}C. Diffraction measurements were made on a Bruker X8 Kappa APEX II Charge-Coupled Device (CCD) area-detector diffractometer using graphite-monochromated Mo Kα radiation. Important crystallographic data are listed in Table S1. The structures were solved by direct methods using SHELXS-97 and refined by full-matrix least-squares techniques on F^2 with SHELXL-97.[5] All H atoms were located by difference maps and were refined isotropically or were introduced at calculated positions as riding on their respective atoms. All non-H atoms were refined anisotropically.

Further experimental crystallographic details for **1**·0.7EtOH: $2\theta_{max}$ = 128°; reflections collected/unique/used, 36381/9690 (R_{int} = 0.0414)/9690; 927 parameters refined; $(\Delta/\sigma)_{max}$ = 0.004; $(\Delta\rho)_{max}/(\Delta\rho)_{min}$ = 0.922/-0.544 e Å^{-3}; R_1/wR_2 (for all data) = 0.0824/0.2073.

Further experimental crystallographic details for **2**·2DMF: $2\theta_{max}$ = 130°; reflections collected/unique/used, 21294/5057 (R_{int} = 0.0381)/5057; 491 parameters refined; $(\Delta/\sigma)_{max}$ = 0.002; $(\Delta\rho)_{max}/(\Delta\rho)_{min}$ = 0.570/-0.457 e Å^{-3}; R_1/wR_2 (for all data) = 0.0542/0.1146.

Further experimental crystallographic details for **3**·6EtOH: $2\theta_{max}$ = 50°; reflections collected/unique/used, 52633/6987 (R_{int} = 0.0379)/6987; 620 parameters refined; $(\Delta/\sigma)_{max}$ = 0.006; $(\Delta\rho)_{max}/(\Delta\rho)_{min}$ = 1.355/-0.646 e Å^{-3}; R_1/wR_2 (for all data) = 0.0369/0.0752.

---

[4] Rigaku/MSC (2005). *CrystalClear*. Rigaku/MSC Inc., The Woodlands, Texas, USA.

[5] G. M. Sheldrick, *Acta Crystallogr.*, 2008, **A64**, 112.

Table S1. Crystallographic data for complexes **1**·0.7EtOH, **2**·2DMF and **3**·6EtOH

	1·0.7EtOH	**2**·2DMF	**3**·6EtOH
Formula	$C_{65.4}H_{72.2}N_4Ni_4O_{12.7}$	$C_{68}H_{72}N_8Ni_4O_{12}$	$C_{76}H_{92}Cl_4N_4Ni_4O_{22}$
Fw	1352.31	1428.18	1790.18
Space group	P-1	P-1	P-1
a (Å)	12.0042(2)	11.3987(2)	11.0498(6)
b (Å)	14.6854(3)	11.9871(2)	11.4157(6)
c (Å)	18.3859(3)	12.9916(2)	17.5861(10)
α (°)	94.749(1)	63.724(1)	99.067(2)
β (°)	95.553(1)	82.282(1)	94.192(3)
γ (°)	105.146(1)	81.803(1)	113.463(2)
V (Å^3)	3094.15(10)	1570.38(5)	1986.76(19)
Z	2	1	1
T (K)	160(2)	160(2)	150(2)
Radiation	Cu Kα	Cu Kα	Mo Kα
ρ_{calcd} (g cm^{-3})	1.451	1.510	1.496
μ (mm^{-1})	1.908	1.925	1.143
Reflections [$I>2\sigma(I)$]	7126	4022	6410
R_1[a]	0.0639	0.0412	0.0326
wR_2[a]	0.1741	0.1035	0.0732

[a] $w=1/[\sigma^2(F_o^2)+(\alpha P)^2+bP]$ and $P = [\max(F_o^2,0)+2F_c^2]/3$,

$R_1 = \Sigma(|F_o|-|F_c|)/\Sigma(|F_o|)$ and $wR_2 = \{\Sigma[w(F_o^2-F_c^2)^2]/\Sigma[w(F_o^2)^2]\}^{1/2}$.

Table S2. Selected Interatomic Distances (Å) and Angles (°) for Complex **1**·0.7EtOH

Ni1-O1	2.057(3)	Ni3-O1	2.099(3)
Ni1-O2	1.956(3)	Ni3-O5	2.059(3)
Ni1-O3	2.239(3)	Ni3-O6	1.968(3)
Ni1-O7	2.029(3)	Ni3-O7	2.206(3)
Ni1-O10	2.101(3)	Ni3-O12	2.103(3)
Ni1-N1	1.968(4)	Ni3-N3	1.987(4)
Ni2-O1	2.205(3)	Ni4-O3	2.095(3)
Ni2-O3	2.049(3)	Ni4-O5	2.218(3)
Ni2-O4	1.969(3)	Ni4-O7	2.052(3)
Ni2-O5	2.035(3)	Ni4-O8	1.975(3)
Ni2-O11	2.122(3)	Ni4-O9	2.073(3)
Ni2-N2	1.971(4)	Ni4-N4	1.993(4)
Ni1…Ni2	3.327(1)	Ni2…Ni3	3.103(2)
Ni1…Ni3	3.068(2)	Ni2…Ni4	3.093(2)
Ni1…Ni4	3.116(2)	Ni3…Ni4	3.297(2)
Ni1-O1-Ni2	102.6(1)	Ni2-O1-Ni3	92.3(1)
Ni1-O1-Ni3	95.2(1)	Ni2-O3-Ni4	96.5(1)
Ni1-O3-Ni2	101.6(1)	Ni2-O5-Ni3	98.6(1)
Ni1-O3-Ni4	91.9(1)	Ni2-O5-Ni4	93.2(1)
Ni1-O7-Ni3	92.7(1)	Ni3-O5-Ni4	100.8(1)
Ni1-O7-Ni4	99.6(1)	Ni3-O7-Ni4	101.4(1)

Table S3. Selected Interatomic Distances (Å) and Angles (°) for Complex **2**·2DMF[a]

Ni1-O1	2.023(2)	Ni2-O1	2.027(2)
Ni1-O2′	2.026(2)	Ni2-O2	2.001(2)
Ni1-O3	2.075(2)	Ni2-O3	2.128(2)
Ni1-O4	1.914(2)	Ni2-O3′	2.075(2)
Ni1-N2	1.989(2)	Ni2-O5	2.085(2)
Ni1…Ni1′	5.282(3)	Ni2-N1	1.985(2)

Ni1…Ni2	3.106(3)	Ni2…Ni2′	3.204(3)
Ni1…Ni2′	3.071(3)		
Ni1-O1-Ni2	100.2(1)	Ni1-O3-Ni2′	95.5(1)
Ni1-O2′-Ni2′	99.4(1)	Ni2-O3-Ni2′	99.4(1)
Ni1-O3-Ni2	95.3(1)		

[a] Symmetry code: (′) = 1-*x*, 2-*y*, -*z*

Table S4. Selected Interatomic Distances (Å) and Angles (°) for Complex **3**·6EtOH[a]

Ni1-O1	2.056(2)	Ni2-O1	2.104(2)
Ni1-O2	2.016(2)	Ni2-O11	1.973(2)
Ni1-O11	2.102(2)	Ni2-O12	2.028(2)
Ni1-O13′	2.074(2)	Ni2-O12′	2.067(2)
Ni1-O21	2.105(2)	Ni2-O22	2.135(2)
Ni1-N1	2.037(2)	Ni2-N11	2.005(2)
Ni1…Ni1′	7.622(3)	Ni1…Ni2′	4.994(1)
Ni1…Ni2	3.008(3)	Ni2…Ni2′	3.142(5)
Ni1-O1-Ni2	92.6(1)	Ni2-O12-Ni2′	100.2(1)
Ni1-O11-Ni2	95.1(1)		

[a] Symmetry code: (′) = 1-*x*, 1-*y*, -*z*

Table S5. Hydrogen Bonds in the Crystal Structure of **1**·0.7EtOH

Interaction	D…A (Å)	H…A (Å)	D-H…A (°)	Symmetry operation
O9-H(O9)…O2	2.688	1.920	151.5	*x*, *y*, *z*
O10-H(O10)…O6	2.649	1.889	149.8	*x*, *y*, *z*
O11-H(O11)…O8	2.763	1.992	152.2	*x*, *y*, *z*
O12-H(O12)…O4	2.737	2.083	134.4	*x*, *y*, *z*
O1E[a]…O8	2.948			*x*, *y*, *z*

[a] O1E is the oxygen atom of the lattice EtOH molecule. A = acceptor, D = donor.

Table S6. Hydrogen Bonds in the Crystal Structure of **3**·6EtOH

Interaction[a]	D…A (Å)	H…A (Å)	D-H…A (°)	Symmetry operation
O21-H(O21)…O25	2.782	2.001	174.9	*x*, *y*, *z*
O22-H(O22)…O1	2.930	2.184	162.4	1-*x*, 1-*y*, -*z*
O23-H(O23)…O2	2.948	2.162	162.6	*x*, *y*, *z*
O24-H(O24)…O3	2.805	1.862	161.6	*x*, *y*, *z*
O25-H(O25)…O3	2.793	1.946	166.5	*x*, *y*, *z*

[a] O21 and O22 are the oxygen atoms of the crystallographically independent, coordinated EtOH molecules (Fig. 3), while O23, O24 and O25 are the oxygen atoms of the crystallographically independent, lattice EtOH molecules. A = acceptor, D = donor.

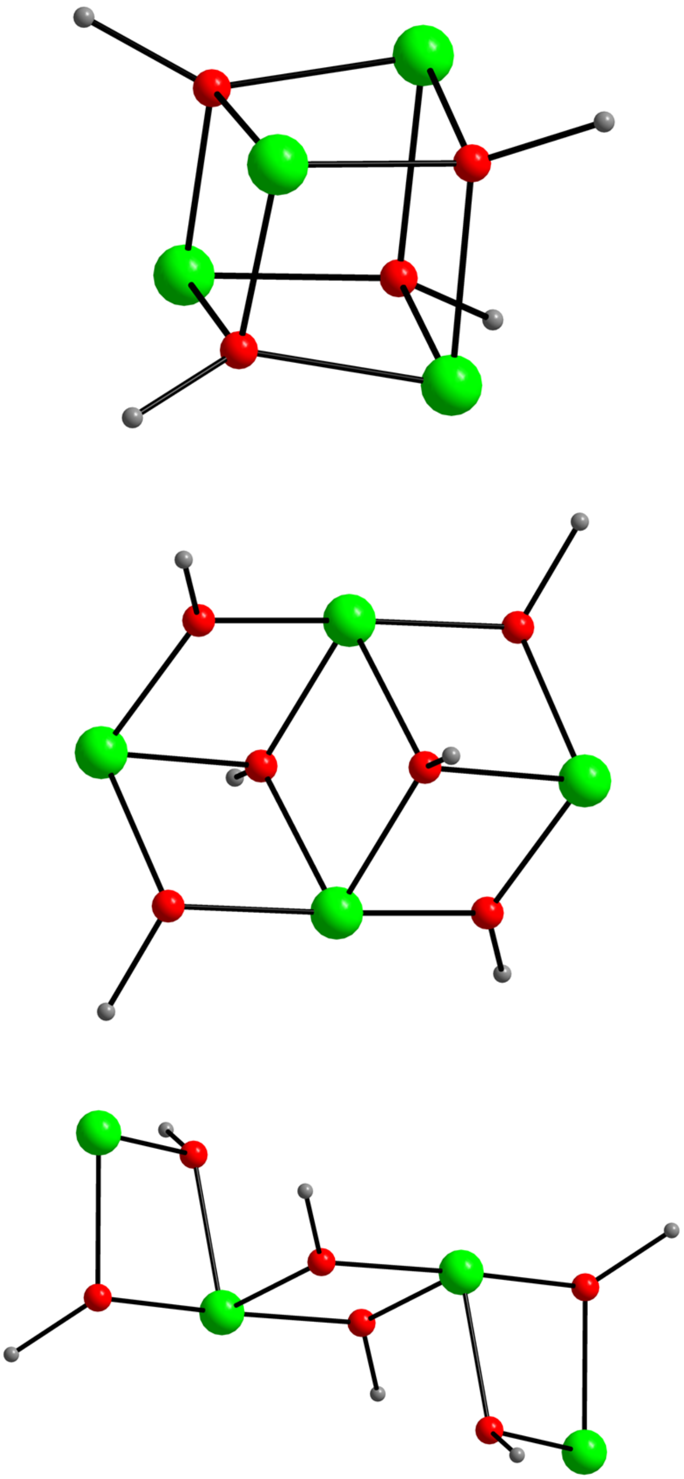

Fig. S1. The $\{Ni_4(\mu_3\text{-}OR)_4\}^{4+}$ cubane (top), $\{Ni_4(\mu_3\text{-}OR)_2(\mu\text{-}OR)_4\}^{2+}$ defective-dicubane (middle), and $\{Ni_4(\mu\text{-}OR)_6\}^{2+}$ zigzag (bottom) cores of complexes **1**, **2**, and **3**, respectively. Color scheme: Ni^{II} green, O red, C gray.

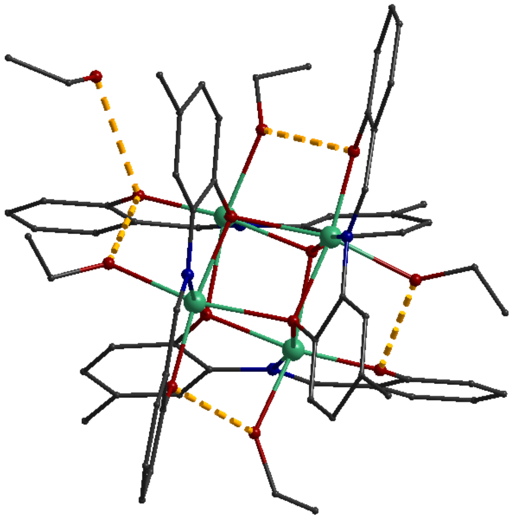

Fig. S2. The H bonds that are present in the crystal structure of **1**·0.7EtOH. There are four intramolecular H bonds with the oxygen atoms of coordinated EtOH ligands as donors and phenolate oxygen atoms (one from each ligand) as acceptors. There is also a possible H bond between the solvate EtOH molecule and one phenolate oxygen.

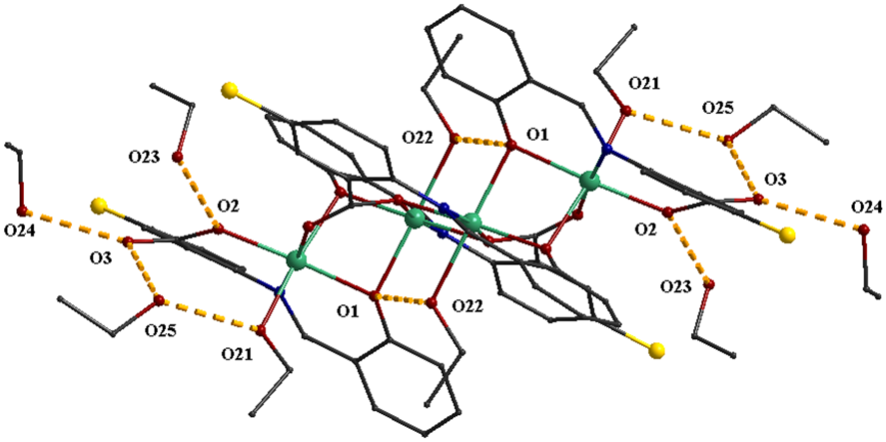

Fig. S3. The H bonds that are present in the crystal structure of **3**·6EtOH. Identical labels (and not primes as in Fig. 3) are used for the symmetry-related atoms. There are two intramolecular H bonds with the oxygen atoms O22 of coordinated EtOH ligands as donors and the phenolate oxygen atoms O21 as acceptors. The rest H bonds are developed between the oxygen atoms O21 (that belong to coordinated EtOH ligands) and O23, O24, O25 (that belong to lattice EtOH molecules) as donors, and the solvate EtOH oxygen atom O25 and the carboxylate atoms O2 and O3 as acceptors.

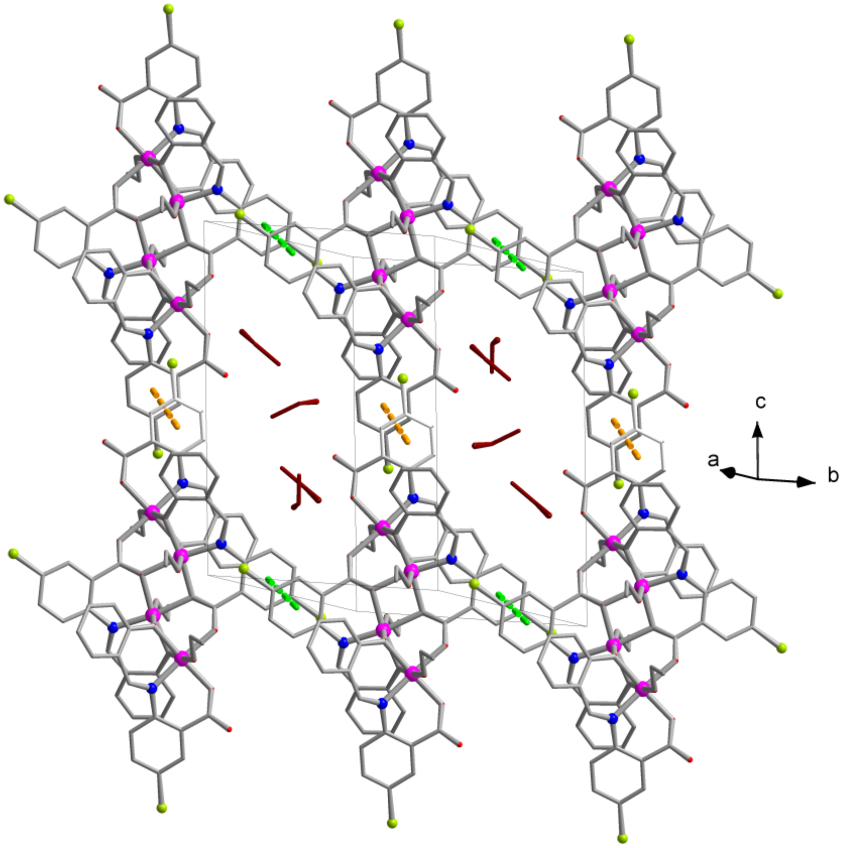

Fig. S4. A small part of the 2-D network of complex **3** formed by the presence of π-π stacking interactions between the aromatic rings of sacb^{2-} ligands. Bright-green dashed lines indicate the interactions developed between C8···C13 rings along *b*-axis and the orange ones indicate the interactions developed between C28···C33 rings along *c*-axis. The lattice EtOH solvate molecules are indicated with dark red lines. As the overlapping rings are centrosymetrically related, their planes are parallel and the inter-centroid distance for the C28···C33 rings is 3.652 Å and for the C8···C13 one 4.062 Å. The EtOH solvate molecules reside in the porous of the 2-D network.

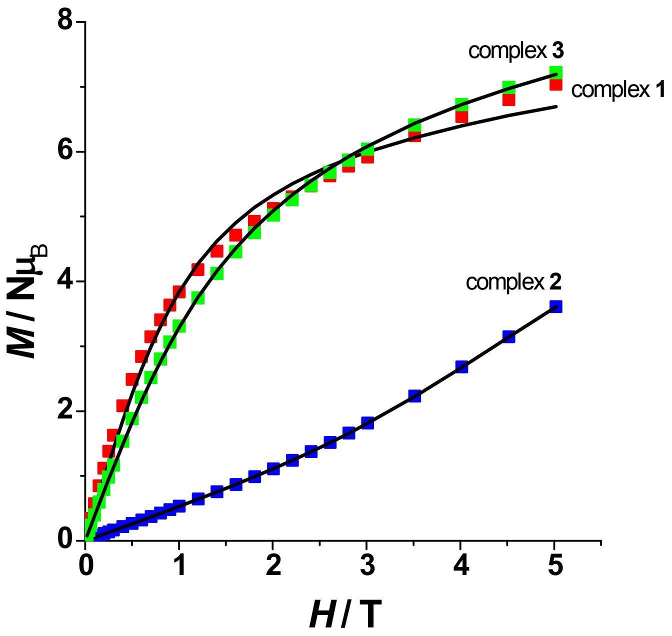

Fig. S5. Plots of magnetization (*M*) *versus* field (*H*) for complexes **1** (red), **2**·DMF (blue) and **3**·2EtOH (green) at 2 K. The solid lines are the fits of the data; see the text for the fit parameters.

MAGNETIC DISCUSSION RELATED TO THE FITTING PROCESS

The acquisition of dc magnetic susceptibility measurements under two different magnetic fields above and below 30 K is simply our routine magnetic "platform" for reasons mentioned in the main text (i.e., to avoid saturation effects). The measurement under a medium-strength field (i.e., 0.3 T) gives better quality plots due to the larger paramagnetic signal, especially if the amount of sample for magnetic studies is small. However, this type of measurement setup cannot be considered as fully accurate when applied at the low temperature regime (< 30 K) for the following reasons/factors: (i) the system is ferromagnetic and we are not in the linear region of magnetization in which the formula χ_M = M/H can be applied, (ii) the system has an appreciable D, and (iii) very importantly, the system has low-lying spin states very close to the ground state;

in such cases the χ_M value could be clearly different under different fields. If any of these factors is present it can be easily detected from preliminary magnetic scans and we thus employ the low-field "model" (i.e., 0.03 T) below 30 K. If the system is clearly anisotropic and we are in the linear region of magnetization, the data under different fields are superimposable and we employ the high-field "model". In every case, we include the corresponding fields in the PHI fit procedure. For compounds **1**-**3** we have employed the low-field "model".

Additional magnetic discussion for the zigzag complex **3**

Applying the *J* values (without *D*) obtained from the magnetization fit, the resulting spin states, their energies and populations at 2 K are listed below:

Spin	**Energy (cm^{-1})**	**Population (%)**
2	0	22.21
3	0.75961E-03	22.20
1	0.88859E-01	20.84
0	0.14973E+00	19.95
4	0.56452E+00	14.80